A&A manuscript no. (will be inserted by hand later)		ASTRONOMY
Your thesaurus codes are: 10 (08.02.7; 08.08.1; 08.16.3; 10.07.3 NGC 6229	9; 10.07.3 M 5)	ASTROPHYSICS

The outer-halo globular cluster NGC 6229. III. Deep CCD photometry

- J. Borissova¹, M. Catelan^{2*,**}, F. R. Ferraro³, N. Spassova¹, R. Buonanno⁴, G. Iannicola⁴, T. Richtler^{5***}, and A. V. Sweigart²
- ¹ Institute of Astronomy, Bulgarian Academy of Sciences, 72 Tsarigradsko chaussèe, BG-1784 Sofia, Bulgaria e-mail: jura@haemimont.bg
- NASA Goddard Space Flight Center, Code 681, Greenbelt, MD 20771, USA e-mail: catelan@stars.gsfc.nasa.gov, sweigart@bach.gsfc.nasa.gov
- Osservatorio Astronomico di Bologna, via Zamboni 33, I-10126 Bologna, Italy e-mail: ferraro@astbo3.bo.astro.it
- Osservatorio Astronomico di Roma, I-00040 Monte Porzio Catone, Italy e-mail: buonanno@astrmp.mporzio.astro.it, iannicola@coma.mporzio.astro.it
- ⁵ Sternwarte der Universität Bonn, Auf dem Hügel 71, D-53121 Bonn, Germany e-mail: richtler@astro.uni-bonn.de

Received; accepted

Abstract. Deep BV photometry for a large field covering the outer-halo globular cluster NGC 6229 is presented. For the first time, a colour-magnitude diagram (CMD) reaching below the main sequence turnoff has been obtained for this cluster. Previous results regarding the overall morphology of the horizontal and giant branches are confirmed. In addition, nine possible extreme horizontal-branch stars have been identified in our deep images, as well as thirty-three candidate blue stragglers. We also find the latter to be more centrally concentrated than subgiant branch stars covering the same range in V magnitude.

A comparison of the cluster CMD with the M 5 (NGC 5904) ridgeline from Sandquist et al. (1996) reveals that:

- i) NGC 6229 and M 5 have essentially identical metallicities;
- ii) NGC 6229 and M 5 have the same ages within the errors in spite of their different horizontal-branch morphologies.

Key words: Stars: blue stragglers – Stars: Population II – Stars: Hertzsprung-Russell (HR) diagram – Galaxy: globular clusters: individual: NGC 6229 – Galaxy: globular clusters: individual: M 5

1. Introduction

NGC 6229 (C1645+476) is one of the most remote globular clusters (GCs) associated with the Galaxy, lying about 30 kpc from the Galactic center (Harris 1996). This outerhalo GC was studied photometrically by Cohen (1986) and Carney et al. (1991) and, more recently, by Borissova et al. (1997, hereafter BCSS97), who presented CCD photometry of the central part of this mildly concentrated GC (c=1.6). In none of these studies, however, was the turnoff (TO) point of the cluster clearly reached, so that no conclusions regarding its age could be made.

As discussed extensively in the two previous papers of this series (BCSS97; Catelan et al. 1998), NGC 6229 shows both a "gap" on the blue horizontal branch (HB) and HB bimodality – unique characteristics among outerhalo GCs. As argued by many authors, an understanding of the nature of the detected peculiarities in "bimodal" and "gap" clusters would be of paramount importance for clarifying the nature of the so-called second-parameter phenomenon (e.g., Buonanno et al. 1985; Catelan et al. 1998; Ferraro et al. 1998; Rood et al. 1993; Stetson et al. 1996; Sweigart 1999; Sweigart & Catelan 1998). Since age is one of the most prominent second-parameter candidates (e.g., Chaboyer et al. 1996b), and since it has been suggested that the outer-halo GC system is younger than the inner-halo one, obtaining deep photometry below the turnoff in NGC 6229 is clearly of considerable interest. For recent discussions on the ages of outer-halo GCs – specifically, NGC 2419, Palomar 3, Palomar 4, Palomar 14, and Eridanus – the reader is referred to Harris et al. (1997), Sarajedini (1997), Stetson et al. (1999), Catelan (1999), and VandenBerg (1999a, 1999b).

Send offprint requests to: J. Borissova

^{*} Hubble Fellow.

 $^{^{\}star\star}$ Visiting Scientist, Universities Space Research Association.

^{***} Visiting Astronomer, German-Spanish Astronomical Center, Calar Alto, operated by the Max Planck-Institut für Astronomie jointly with the Spanish National Commission for Astronomy.

In this paper we present, for the first time, deep BV photometry reaching below the NGC 6229 TO level. Our observational material and data reduction techniques are described in Sect. 2 together with our analysis of the photometric errors and completeness corrections. Several aspects of the colour-magnitude diagram (CMD) of NGC 6229 including candidate blue straggler and extreme HB stars are described in Sect. 3. The metallicity of NGC 6229, as determined from various photometric indicators, and its age relative to M 5, as derived from a differential application of both the "vertical" and "horizontal" methods, are then discussed in Sects. 4 and 5, respectively. In Sect. 6 we summarize the most important results of the present investigation.

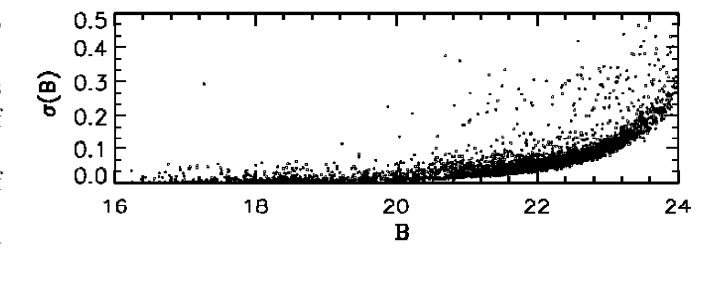
In the next paper of this series, a detailed investigation of the RR Lyrae population in NGC 6229 will be provided.

2. Observations

2.1. CCD photometry

Our analysis is based on the following observational material:

- 1. A large set of CCD frames obtained on the nights of August 25-26 1987, at the Calar Alto observatory (Spain) of the Max-Plank Institute für Astronomie (Heidelberg), using the 3.5m telescope equipped with a 1032×624 RCA chip (hereafter "CA dataset"). The array scale was 0.25" pixel⁻¹, giving a field of view of about $4.3' \times 2.6'$. Only the nine frames with the best seeing (FWHM better than 1") were used to obtain the deep photometry down to V=24 mag presented in this paper. Three partially overlapping fields, covering a total area of $\sim 22 \,\mathrm{arcmin}^2$ around the cluster center, were observed during the run. However, only short exposures ($\sim 10 \, \mathrm{sec}$) were obtained in the field centered on the cluster center, while long exposures (ranging from $\sim 1000 \, \text{sec}$ up to $1300 \, \text{sec}$) were secured only in the two more external fields placed at $\sim 2'$ North-West and South-West with respect to the cluster center.
- 2. Fifty-four B,V frames obtained on June 28-30 1997, plus six B,V frames obtained on October 6-8 1997 at the 2m Ritchey-Chrétien telescope of the Bulgarian National Astronomical Observatory "Rozhen" with a Photometrics 1024×1024 CCD camera (hereafter "Rozhen dataset"). The seeing during these observations was $\approx 1''$ with stable and very good photometric conditions. The scale at the Cassegrain-focus CCD was 0.33'' pixel $^{-1}$ and the observing area was $5.6' \times 5.6'$, centered on the cluster center. Ten B and 10~V frames obtained under the best photometric conditions were added up, resulting in total exposure times of 1260 sec and 1200 sec, respectively. Two standard fields of M 67 (Christian et al. 1985) were taken before and after the observations, for calibration purposes.



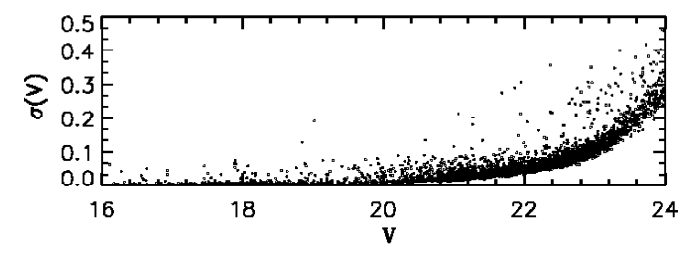


Fig. 1. Formal errors of the Rozhen photometry from the DAOPHOT package as a function of the mean B and V magnitudes for each star

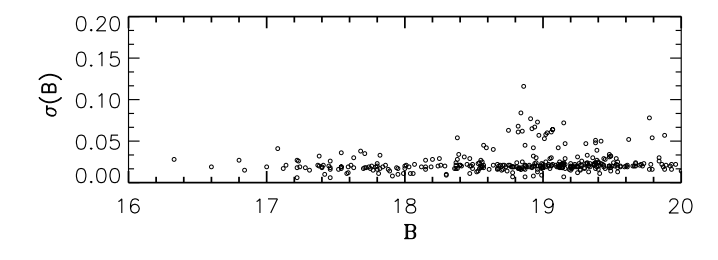
2.2. Data reduction

The stellar photometry of the frames was carried out independently using ROMAFOT (Buonanno et al. 1983) for the CA dataset and DAOPHOT/ALLSTAR (Stetson 1993) for all other frames. Instrumental magnitudes were determined for 1500 – 5000 stars on each frame.

The instrumental values of all the "Rozhen" frames were transformed to the standard system using the standard field in M67 (Christian et al. 1985). Due to unfavorable weather conditions during the CA run, no independent photometric calibration was possible for the CA dataset. For this reason, the magnitudes of this sample were originally referred to the B, V Johnson system using a large set of stars in common with Carney et al. (1991). In order to check the compatibility of the magnitude systems of the two datasets, we adopted the following procedure: we first transformed the Rozhen x, y coordinate system to the CA local system and then searched for stars in common between the two datasets – resulting in a sample of more than 900 stars. The residuals in magnitude and colour for the stars in common do not show any systematic difference or trend so we can conclude that the two datasets are homogeneous in magnitude within the errors. This result also suggests that the calibration obtained for the Rozhen dataset and adopted for the whole dataset presented in this paper nicely agrees with the Carney et al. (1991) zero point.

2.3. Photometric errors

In order to estimate the internal accuracy of our CCD measurements for the Rozhen dataset, we used the formal errors from the DAOPHOT package and the rms



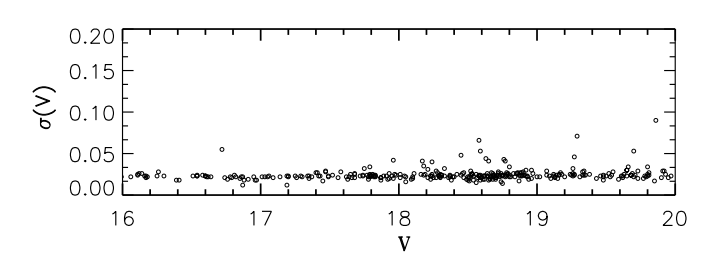


Fig. 2. Rms frame-to-frame scatter of the instrumental magnitudes from the Rozhen photometry as a function of the mean B and V magnitudes for each star

frame-to-frame scatter of the instrumental magnitudes. The formal errors for all stars vs. their magnitudes are displayed in Figure 1. As can be seen, we have large errors (> 0.15 mag) for B > 22.5 mag and V > 23.0 mag, which therefore define the faint limit of the Rozhen photometry (≈ 1.5 mag fainter than the TO point in V).

Following the method described in Ferraro & Paresce (1993), we calculated the rms frame-to-frame scatter of the instrumental magnitudes of the 15 B and V frames from the Rozhen dataset obtained in the same seeing and FWHM. The plot of the rms scatter vs. the mean magnitudes in the B and V filters is given in Figure 2. The mean rms scatter in both filters over the whole magnitude interval is $0.02~{\rm mag}$.

The errors in the CA case, given in Table 1, were determined as the rms scatter of multiple measures of stars observed in the overlapping regions of adjacent fields. Also given in Table 1 are the errors obtained for the Rozhen dataset.

Table 1. The mean standard deviations of the CA and Rozhen datasets

V range	$\sigma(B)_{\mathrm{CA}}$	$\sigma(V)_{\mathrm{CA}}$	$\sigma(B)_{\mathrm{Rozhen}}$	$\sigma(V)_{ m Rozhen}$
14.0 - 20.0	0.02	0.02	0.02	0.01
20.0 - 22.0	0.06	0.06	0.04	0.03
22.0 - 24.5	0.10	0.10	0.12	0.15

The final photometric accuracy for the Rozhen and CA datasets should include all of these error estimates. From the errors given in Figures 1 and 2 and Table 1 we conclude that the total uncertainty is ≈ 0.03 mag for V < 21 mag and B < 21 mag and between 0.05 mag and 0.1 mag for the fainter magnitudes.

Table 2. Completeness functions for the Rozhen dataset

V range	F(B)	F(V)
16.5 - 17.0	1.00	1.00
17.0 - 17.5	1.00	1.00
17.5 - 18.0	1.00	1.00
18.0 - 18.5	1.00	1.00
18.5 - 19.0	1.00	1.00
19.0 - 19.5	1.00	1.00
19.5 - 20.0	1.00	1.00
20.0 - 20.5	0.99	1.00
20.5 - 21.0	0.96	0.97
21.0 - 21.5	0.92	0.94
21.5 - 22.0	0.86	0.88
22.0 - 22.5	0.69	0.74
22.5 - 23.0	0.55	0.61
23.0 - 23.5	0.38	0.44
23.5 - 24.0	0.18	0.24
24.0 - 24.5	0.06	0.10

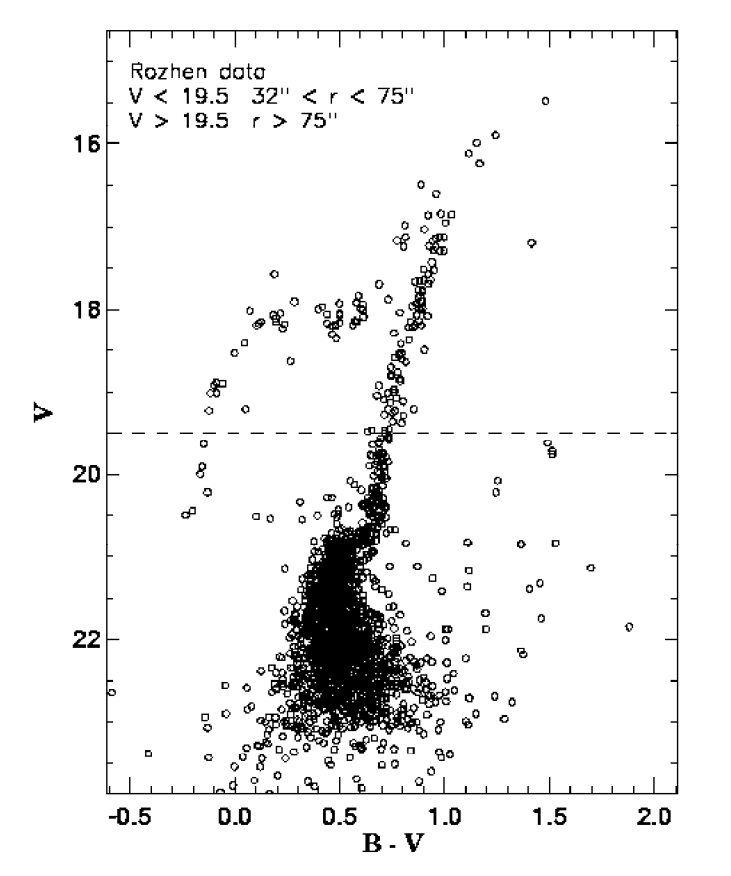
2.4. Completeness corrections

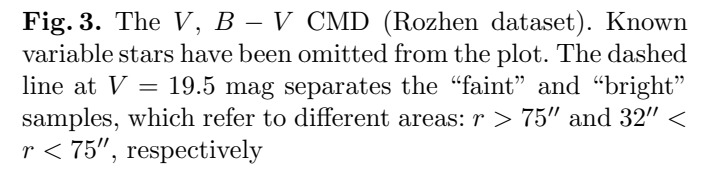
The last step in our data reduction was to determine the completeness functions in the B and V filters. We used the artificial star technique (Stetson & Harris 1988; Stetson 1991a, 1991b) to create a series of artificial frames by means of the ADDSTAR routine in DAOPHOT II. These artificial frames were then re-reduced in the same manner as the original frames to obtain the completeness functions F(B) and F(V), defined as the ratio of recovered to added artificial stars. The completeness functions for the Rozhen dataset are listed in Table 2.

Table 3. Number counts for the CA and Rozhen datasets for various evolutionary branches

Branch	CA sample	Rozhen sample	$\frac{N(\mathrm{CA})}{N(\mathrm{Rozhen})}$
MS	234	225	1.04
SGB	236	278	0.85
RGB	31	26	1.19
Red HB	6	7	0.86
RR Lyraes	4	5	0.80
Blue HB	14	10	1.40
AGB	6	6	1.00
BSS	8	7	1.14
Field stars	13	14	0.93

Since no specific artificial star test has been performed on the CA sample, we can compare the relative completeness degree of the two samples from a direct comparison of the star counts found in each evolutionary branch. In doing this we selected an area common to both datasets relatively far from the cluster center (1.0' < r < 1.5'). Then we derived the CMDs over this area for the two samples and counted the number of stars in each branch (with V < 22 mag) uncorrected for completeness. The number of stars for the cluster branches and the ratio be-





tween the numbers found in the CA and Rozhen datasets are given in Table 3. As can be seen, the two samples have very closely the same overall degree of completeness.

3. The Colour-Magnitude Diagram

3.1. Overall CMD morphology

The $V,\,B-V$ CMDs for the Rozhen and CA datasets are presented in Figures 3 and 4, respectively. The following selection criteria were adopted in order to have the best definitions of the CMD branches: for V>19.5 mag, only stars with r>75'' from the cluster center were plotted [we find the subgiant branch (SGB)-TO region to be better defined in this region]; for stars with V<19.5 mag, the annular region with 32''< r<75'' was employed (thus avoiding the crowding in the innermost regions while minimizing field star contamination). In Figure 4 the M 5 (NGC 5904) ridgeline from Sandquist et al. (1996) is overplotted. Vertical and horizontal shifts of $\delta V=3.0$ mag and $\delta (B-V)=0.0$ mag, respectively, have been applied to the M 5 mean ridgelines. The magnitude shift was de-

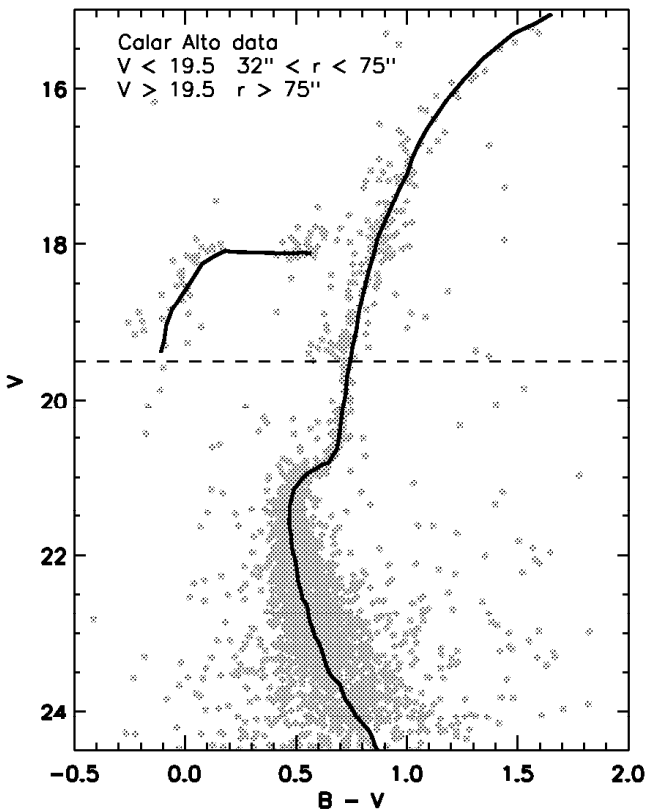


Fig. 4. The V, B-V CMD (CA dataset). Known variable stars have been omitted from the plot. The dashed line at V=19.5 mag separates the "faint" and "bright" samples, which refer to different areas: r>75'' and 32''< r<75'', respectively. The M 5 ridgeline from Sandquist et al. (1996) is overplotted

termined in order to have a good match to the red HB of NGC 6229, while the colour shift was derived by matching the lower RGBs ($V \sim 20$ mag; see Figure 4 and Figure 9a).

The $V,\,B-V$ CMD for 818 stars in common between the Rozhen and CA datasets is presented in Figure 5. To avoid crowding in the innermost regions only stars with r>32'' and V<22 mag have been plotted. Blue straggler stars (BSS) and extreme HB (EHB) candidates (see Sects. 3.3 and 3.4) are plotted as asterisks and filled squares, respectively. From the comparison of Figure 5 with Figures 3 and 4 it is evident that most of these stars are located in the innermost regions (32'' < r < 75'').

Our new CMD generally confirms the previous photometric results of BCSS97. In particular, we can clearly see the presence of both a red giant branch (RGB) and an asymptotic giant branch (AGB) population, besides the bimodal HB with a long blue tail and a "gap" at $V \simeq 18.4$ mag extensively discussed by BCSS97 and Catelan et al. (1998). There is a hint of a second gap, located at $V \simeq 20$ mag, as previously noted by Carney et al. (1991). Importantly, however, we have for the first time clearly

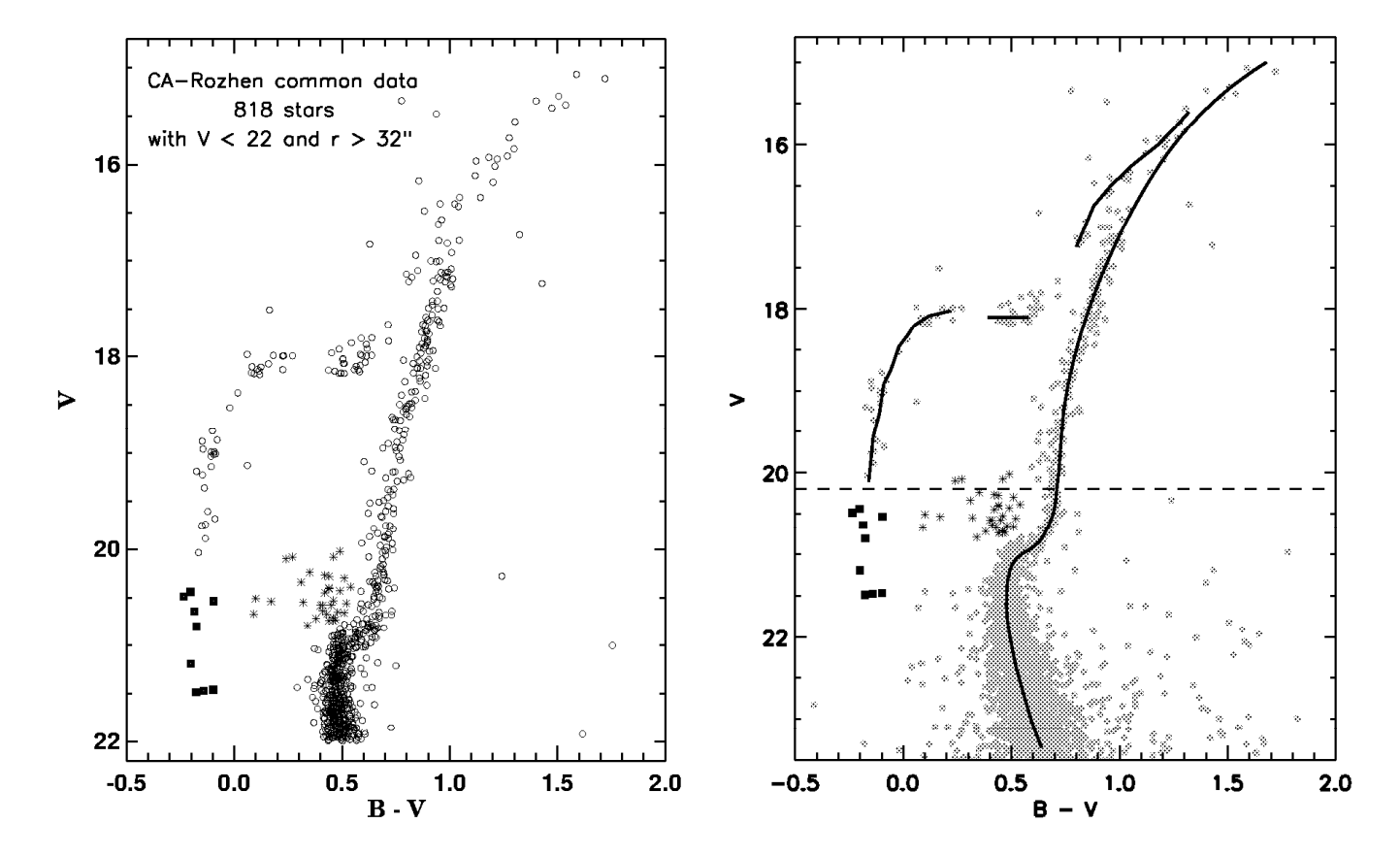


Fig. 5. The V, B-V CMD for stars in common between the Rozhen and CA datasets with V<22 mag and r>32'' (see text). Filled squares denote candidate extreme horizontal-branch stars; asterisks indicate probable blue straggler stars. Known variable stars are omitted from the plot

identified the main-sequence (MS) TO point as well as a population of BSS only hinted at in previous photometric results (see Figure 3 in Carney et al. 1991, and Figure 2 in BCSS97) and a possible extension of the blue-HB tail to the EHB region. Each of these new features will be discussed in the subsections below.

The CMD in Figure 5, augmented by data from the CA dataset for V>22 mag, was used to determine the fiducial lines of the main branches of NGC 6229 by means of a least-squares fit. The best fit of the upper part of the RGB (V<19 mag) was obtained with an equation of the form:

$$V = a + bx + cx \ln x + dx^{0.5} \ln x + e(\ln x)^{2},$$
 (1)

where x = B - V. In determining the free parameters in eq. (1) we rejected stars lying far from the mean branches and suspected field stars during the several iterations. The std. error of the resulting fit is 0.09 mag. The mean ridgelines of the fainter RGB (V > 19 mag), SGB, MS and BHB were determined by dividing these branches into bins

Fig. 6. Detailed plot showing the BSS (asterisks) and EHB (filled squares) candidates in NGC 6229. The fiducial lines of the cluster are overplotted upon the data in common between the two datasets for V < 20.2 mag, and from the CA dataset only (r > 350 pixels) for V > 20.2 mag. The data in this figure (grey circles) are plotted for illustrative purposes only, and are not representative of the actual CMD of NGC 6229. Note the difference in brightness between the red HB and the tip of the blue HB

and computing in each bin the mode of the distribution in colour. Only the CA dataset was used to define the fiducial line of the MS region. Ten stars in common with the Rozhen dataset for which the DAOPHOT parameters SHARP and CHI indicated possible blends were discarded. Table 4 presents the adopted normal points for each branch. The resulting ridgeline is plotted in Figure 6, along with the stars from both the Rozhen and CA datasets employed to obtain such a ridgeline. The 10 possible blends noted above have not been removed from the plot; they all have $V \sim 20.9$ mag, $B-V \sim 0.5$ mag, and can be recognized as a "clumpy" structure immediately below the BSS region in the CMD.

The MS TO point is found to be at $V_{\rm TO}=21.60\pm0.10$ mag and $(B-V)_{\rm TO}=0.48\pm0.05$ mag. The quoted errors are the errors of the fitting procedure. The magnitude level of the HB, determined as the lower boundary of the red HB "clump", is $V_{\rm HB}=18.10\pm0.05$ mag. This

Table 4. Mean fiducial lines of NGC 6229

\overline{V}	B-V	\overline{V}	B-V	\overline{V}	B-V
MS+S	GB+RGB			Red Hl	В
15.00	1.680	18.70	0.781	18.10	0.58
15.10	1.620	18.80	0.772	18.10	0.48
15.20	1.566	18.90	0.764	18.10	0.39
15.30	1.515	19.00	0.757	Blue H	В
15.40	1.469	19.10	0.750	18.02	0.22
15.50	1.426	19.20	0.744	18.08	0.12
15.60	1.386	19.28	0.740	18.13	0.09
15.70	1.349	19.43	0.735	18.20	0.05
15.80	1.315	19.70	0.727	18.32	0.02
15.90	1.283	19.96	0.720	18.46	-0.02
16.00	1.253	20.21	0.709	18.61	-0.04
16.10	1.224	20.39	0.702	18.76	-0.06
16.20	1.197	20.52	0.691	18.91	-0.09
16.30	1.172	20.63	0.675	19.08	-0.10
16.40	1.147	20.77	0.648	19.27	-0.11
16.50	1.124	20.84	0.630	19.57	-0.14
16.60	1.102	20.90	0.606	19.85	-0.15
16.70	1.080	20.95	0.575	20.11	-0.16
16.80	1.059	21.00	0.544	AGB	
16.90	1.039	21.05	0.522	15.60	1.32
17.00	1.020	21.13	0.502	15.75	1.27
17.10	1.001	21.20	0.491	16.00	1.18
17.20	0.983	21.25	0.488	16.25	1.06
17.30	0.966	21.31	0.482	16.50	0.96
17.40	0.949	21.42	0.479	16.75	0.88
17.50	0.932	21.52	0.478	17.00	0.84
17.60	0.916	21.60	0.477	17.25	0.80
17.70	0.901	21.70	0.478		
17.80	0.886	21.80	0.482		
17.90	0.872	21.94	0.489		
18.00	0.858	22.08	0.499		
18.10	0.845	22.23	0.510		
18.20	0.833	22.36	0.521		
18.30	0.821	22.63	0.549		
18.40	0.810	23.02	0.592		
18.50	0.800	23.35	0.638		
18.60	0.790				

implies a magnitude difference between the HB and the TO of $\Delta\,V_{\rm TO}^{\rm HB}=3.50\pm0.11$ mag.

3.2. Number ratios

The conclusions from BCSS97 regarding the $R=N_{\rm HB}/N_{\rm RGB}$ ratio (Iben 1968) between HB stars and RGB stars brighter than the HB are confirmed. Using all the available data (BCSS97, CA and Rozhen), we find the following number counts: $N_{\rm HB}=285$ (including 9 candidate EHB stars; cf. Sect. 3.4 below), $N_{\rm RGB}=258$, and $N_{\rm AGB}=57$. It thus follows that $R=1.10\pm0.10$ ($R=1.07\pm0.10$ excluding the suspected EHB stars). For $R'=N_{\rm HB}/N_{\rm (RGB+AGB)}$, the values are $R'=0.90\pm0.07$ and $R'=0.88\pm0.07$, respectively. Note that the BCSS97 number counts have been corrected for completeness as described therein. We have assumed a differential bolometric

correction between the HB and the RGB of 0.15 mag (Buzzoni et al. 1983). As emphasized by Carney et al. (1991) and BCSS97, these R and R' values for NGC 6229 indicate either a low cluster helium abundance ($Y \approx 0.19$) or the presence of a substantial, but as yet undetected, population of EHB stars (see BCSS97 for more details).

As noted by BCSS97, a low helium abundance for NGC 6229 would lead to a *red* HB morphology, as opposed to what is observed (Figure 5). In fact, there is even a hint of an (extremely hot) EHB population in NGC 6229 (see Sect. 3.4).

Since in Sect. 5 the age of NGC 6229 will be compared with that of M 5, it is important to investigate any possible differences in the chemical composition which could invalidate the comparison. While the discussion of the metal content of the two clusters is presented in Sect. 4, we here compare the R-ratios in NGC 6229 and M 5. In doing this comparison we shall adopt (in order to be fully consistent with Sandquist et al. 1996) their differential bolometric correction between the HB and the RGB, which turns out to be 0.265 mag for the V filter. In this case, we have $N_{\rm RGB} = 275$ and the ratios: $R = 1.04 \pm 0.10$ $(R = 1.00 \pm 0.10), R' = 0.86 \pm 0.07 (R' = 0.83 \pm 0.07).$ These ratios are fully consistent with those obtained by Sandquist et al. for M 5 $(R = 1.12 \pm 0.10, R' = 0.94 \pm 0.09)$ - see their Table 7). From this comparison, it follows that there is no significant difference in R or R' between the two clusters, and that the difference in Y between them is unlikely to be higher than $\delta Y \sim 0.01$.

The consistency of the *R*-ratios derived above would not exclude, however, phenomena such as helium mixing amongst NGC 6229 red giants, which as pointed out by Sweigart (1997) would not affect – to a *first approximation* – the number ratios.

3.3. Blue straggler stars

None of the previous photometric investigations of NGC 6229 (Cohen 1986; Carney et al. 1991; BCSS97) addressed the BSS in the cluster. Fusi Pecci et al. (1992), on the basis of Figure 3 in Carney et al (1991), discussed 13 BSS candidates and accordingly put NGC 6229 in their group "BS3", alongside M3 (NGC 5272). (For a much more detailed discussion of the special BSS population in the latter cluster, see Ferraro et al. 1997.)

Note that the "horizontal" method of relative-age determination is essentially helium abundance-independent (e.g., Bolte 1990). The "vertical" method of age derivation is also weekly dependent on Y, provided the adopted GC distance scale is model-independent – coming, for instance, from the Baade-Wesselink method applied to RR Lyrae variables. It is only in those instances where the helium abundance is consistently used to estimate the HB (and TO) luminosity by means of evolutionary models that the "vertical" method becomes substantially dependent on Y. This topic is discussed at some length in Sect. 4 of Catelan & de Freitas Pacheco (1996).

Table 5. BSS candidates

No.	x	y	V	B-V	Distance (')
1	624.90	75.997	20.27	0.42	0.53
2	355.73	322.37	20.79	0.34	0.64
3	388.20	101.47	20.45	0.42	0.66
4	498.71	176.58	20.67	0.43	0.71
5	384.89	132.75	20.56	0.52	0.75
6	516.62	192.28	20.41	0.44	0.77
7	95.32	291.92	20.02	0.49	0.77
8	510.12	207.09	20.58	0.45	0.83
9	583.30	211.97	20.64	0.41	0.89
10	283.93	351.55	20.08	0.46	0.90
11	498.31	224.24	20.72	0.38	0.90
12	609.89	206.05	20.30	0.51	0.91
13	322.69	122.20	20.74	0.46	0.93
14	482.62	233.90	20.58	0.41	0.95
15	428.56	224.84	20.73	0.47	0.97
c659	276.73	389.97	20.40	0.44	0.88
c420	752.60	66.27	20.74	0.44	1.00
c412	421.42	245.32	20.53	0.46	1.11
c378	239.43	196.50	20.28	0.44	1.39
c481	834.96	131.28	20.71	0.46	1.41
c416	266.20	244.98	20.66	0.51	1.43
c376	202.99	362.55	20.08	0.27	1.43
c460	882.81	49.51	20.51	0.10	1.52
c429	225.37	299.61	20.43	0.49	1.71
c436	93.29	156.11	20.39	0.54	1.86
c478	79.88	257.66	20.54	0.17	2.08
c356	1088.71	99.30	20.34	0.31	2.39
c329	675.01	204.75	20.10	0.24	1.10
c358	452.31	-141.51	20.65	0.48	0.66
c425	601.18	-402.376	20.55	0.32	0.81
c499	454.45	312.57	20.67	0.09	0.74
c327	345.06	241.18	20.24	0.35	1.38
c426	283.54	336.03	20.58	0.40	0.95

In order to identify possible BSS candidates in NGC 6229, we followed the guidelines from Fusi Pecci et al. (1992, 1993). Accordingly, we checked the status of all stars forming an extension of the MS up to about 1.5 mag brighter than the TO point in V, and also the stars located ≈ 0.1 mag redder than the TO. This yielded the thirty-three possible BSS plotted in Figures 5 and 6. All these stars were measured in both the Rozhen and CA datasets. Careful checks were made to ensure that the internal errors of the BSS candidates are the same as those of the subgiants at the same level. The DAOPHOT parameters SHARP and CHI were checked for each BSS candidate, in order to ensure that most are unlikely to be the result of spurious photometric blends (e.g., Ferraro et al. 1992). Follow-up observations are needed to confirm their evolutionary status though.

According to the Galaxy model of Ratnatunga & Bahcall (1985), the predicted number of field stars in our fields [2 stars at 20 < V(mag) < 21 and B - V < 0.8 mag] is not sufficient to explain this population.

Data for the BSS candidates in NGC 6229 – magnitudes, colours and distance from the cluster center – are listed in Table 5. Their x and y coordinates are in the CA coordinate system. Eighteen of these candidates are found in the Carney et al. (1991) photometry list, although only seven (labeled c425, c359, c426, c358, c460, c376 and c478 in Table 5) were selected by Fusi Pecci et al. (1992, 1993). We were unable to identify their remaining candidates, possibly due to the large errors reported by Carney et al. (1991). Our BSS candidates are shown in Figures 5 and 6.

The implied "specific frequency" of BSS in NGC 6229 (at r > 32'') is

$$F_{\rm HB}^{\rm BSS} = \frac{N_{\rm BSS}}{N_{\rm HB}} \simeq 0.19. \tag{2}$$

This should be compared with the overall frequencies recently obtained with HST for a series of GCs: 0.17 for M 13 (NGC 6205); 0.67 for M 3; and ~ 1 for M 80 (NGC 6093) (Ferraro et al. 1999b). This would suggest a similar specific frequency of BSS between NGC 6229 and M13. Note that both M 13 and NGC 6229 are not dynamically evolved (e.g., Trager et al. 1995), as opposed to what is likely to be the case for M 80 – whose core is indeed trying to collapse and stellar interactions may be preventing this from happening. The extremely large specific frequency of BSS in M 80 is likely to be due to this effect (Ferraro et al. 1999b).

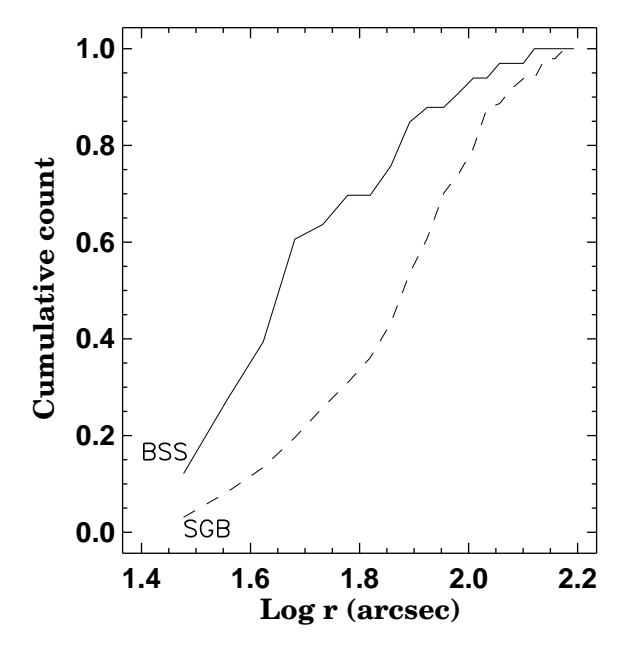


Fig. 7. Radial cumulative distributions of the candidate BSS (solid line) and SGB stars (dashed line) in NGC 6229

We mention, however, several caveats in comparing the above HST $F_{
m HB}^{
m BSS}$ values with our ground-based value for

NGC 6229 (see also Ferraro et al. 1995). In particular, the samples employed to obtain the NGC 6229 and the HST specific frequencies are:

- a) Heterogeneous in sampling: the HST surveys are obtained in the very central region of each cluster, whereas the NGC 6229 $F_{\rm HB}^{\rm BSS}$ value has been derived for its external region (r>32'');
- b) Heterogeneous in photometric filters and accuracy: the BSS samples in HST surveys are based on ultraviolet filters which are much more efficient than B and V (as used here) for obtaining complete BSS samples;
- c) Heterogeneous in defining the "lower edge" of the BSS sample: due to the different filter systems, it is unclear whether the (somewhat arbitrary) lower edges coincide in the HST ultraviolet and ground-based B,V studies, possibly introducing an important systematic bias.

We thus caution that the above comparison among HST $F_{\rm HB}^{\rm BSS}$ values and NGC 6229's might be substantially modified once high-accuracy HST data in the ultraviolet are available for NGC 6229.

Systematic differences in the radial distribution of BSS with respect to SGB stars spanning the same magnitude range have been detected in many GCs (I. Ferraro et al. 1995). The radial distribution of the 33 BSS listed in Table 5 was compared with the one for 97 SGB stars lying within ± 0.1 mag in B-V from the cluster fiducial line over the magnitude range 20 < V(mag) < 21. The cumulative radial distributions for both samples are plotted in Figure 7 as a function of the projected distance from the cluster center (r > 32''). It is evident from this plot that the candidate BSS (solid line) are more centrally concentrated than the SGB stars (dashed line). A Kolmogorov-Smirnov test applied to the two distributions shows that the possible BSS population in NGC 6229 is more centrally concentrated than the SGB population in the same magnitude interval with 96 % confidence.

Figure 8 presents the NGC 6229 BSS luminosity function (LF). This LF seems consistent with the total LF presented by Fusi Pecci et al. (1992, 1993) for 625 BSS in 25 GCs, displaying a peak at $M_V \simeq 3.2$ mag. It is not possible to tell, on the basis of our data alone, whether NGC 6229's BSS LF is fully compatible with the "global" LF for GCs with $\rho_0 > 10^3 \, M_{\odot} \, \mathrm{pc}^{-3}$, which appears to differ from the one for GCs of lower central density (cf. Figure VIII in Fusi Pecci et al. 1993). For comparison purposes, we display in Figure 8 the overall LF for BSS in a set of seven GCs with $\rho_0 > 10^3 \, M_{\odot} \, \mathrm{pc}^{-3}$ from Fusi Pecci et al. (1993) (dashed line), after removing NGC 6229 and M3 from their sample. For NGC 6229, $\rho_0 \simeq 2.5 \times 10^3 \, M_{\odot} \, \mathrm{pc}^{-3}$. Note that, for consistency, the distance modulus $[(m-M)_V = 17.31 \text{ mag}]$ and E(B-V) = 0.01 mag] and metallicity scales adopted when producing Figure 8 were the same as in Fusi Pecci et al. (1993).

Since NGC 6229 is a crowded, mildly concentrated outer-halo GC, HST imaging will definitely be necessary

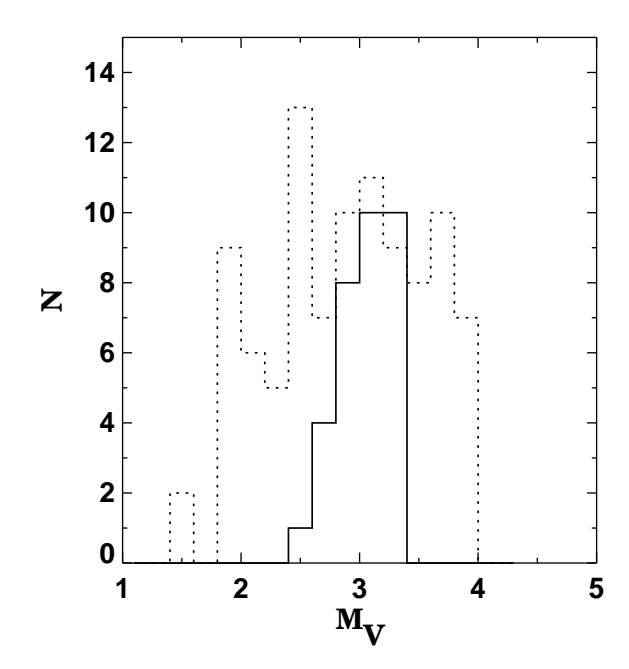


Fig. 8. Luminosity function of the candidate BSS in NGC 6229 (solid line), compared with that for seven GCs with $\rho_0 > 10^3 \, M_{\odot} \, \mathrm{pc}^{-3}$ from Fusi Pecci et al. (1993) (dashed line)

in order for a likely centrally concentrated BSS population to be positively identified in its innermost regions.

3.4. Extreme HB stars

The putative extreme HB (EHB) population suggested by BCSS97 could not be unquestionably identified in the present study, although we found strong hints that it may indeed be present. The implications of the presence (or otherwise) of an EHB population in NGC 6229 have been discussed at length by BCSS97 and Catelan et al. (1998).

There are nine stars (marked by filled squares in Figures 5 and 6) reaching as faint as V = 21.4 mag, and having $B-V \approx -0.15$ mag, which resemble an EHB extension to the long blue HB tail of NGC 6229. Magnitudes, colours and distances from the cluster center for these stars are listed in Table 6. Unfortunately, most of these stars are identified only on the CA dataset in the high crowding region and have relatively large photometric errors. Two of them, however (No. 5 and c397 in Table 6), were also measured in the Rozhen dataset, their photometric parameters being in very good agreement between the two datasets. We identify star No. 397 in the Carney et al. (1991) photometry list as an EHB candidate. Accurate photometry extending to even fainter magnitudes is necessary to confirm their nature. In particular, in order to identify a possible prominent EHB population in NGC 6229 (see BCSS97), HST photometry reaching the very crowded cluster core will be required. We recall that the conspic-

Table 6. Extreme HB candidates

No.	x	y	V	B-V	Distance $(')$
1	562.545	86.141	20.642	-0.185	0.382
2	458.270	100.294	20.535	-0.097	0.459
3	389.157	59.478	21.192	-0.201	0.572
4	458.255	141.58	20.803	-0.176	0.611
5	322.760	304.384	20.490	-0.235	0.880
6	621.255	179.482	21.462	-0.098	0.839
7	473.597	223.595	21.485	-0.177	0.919
8	279.580	344.230	21.471	-0.142	0.951
c397	675.420	309.552	20.441	-0.203	2.077

uous EHB population in the core of NGC 2808, a much closer GC ($R_{\odot} = 9.3$ kpc, compared to $R_{\odot} = 29.3$ kpc for NGC 6229 – data from Harris 1996), was *only* discovered using HST (Sosin et al. 1997), notwithstanding the fact that deep ground-based CCD photometry had already been published for the outer regions of NGC 2808 (Ferraro et al. 1990).

4. Metallicity

We can derive a *photometric* estimate of the cluster metallicity from the absolute location in colour of the RGB and from its overall morphology. Many observational photometric indicators have been proposed and calibrated for this purpose. In the following we will use:

- $(B-V)_{0,g}$, defined by Sandage & Smith (1966) as the RGB dereddened colour at the HB luminosity level;
- $\Delta V_{1.4}$, defined by Sandage & Wallerstein (1960) as the magnitude of the RGB at $(B-V)_0=1.4$ mag with respect to the HB level. Similar parameters $\Delta V_{1.1}$ and $\Delta V_{1.2}$, measured at $(B-V)_0=1.1$ mag and $(B-V)_0=1.2$ mag, respectively, have been recently defined by Sarajedini & Layden (1997);
- $(B-V)_{0,-2}$, defined by Sarajedini & Layden (1997) as the RGB colour at $M_V = -2$ mag;
- S, defined by Hartwick (1968) as the slope of the RGB measured between two points along the RGB: the first at $V_{\rm HB}$ and the second at $V=V_{\rm HB}-2.5\,{\rm mag}$;
- $\Delta V_{\mathrm{bump}}^{\mathrm{HB}}$, the location of the RGB "bump" in the CMD relative to the HB level. A recalibration of this indicator as a function of cluster metallicity has been recently provided by Sarajedini & Forrester (1995), expanding on the dataset used in the original calibration (Fusi Pecci et al. 1990).

In order to measure these parameters for NGC 6229, we first need to adopt values for the interstellar reddening, distance modulus and $V_{\rm HB}$. For consistency with the values used in the previous sections (except for Sect. 3.2), we will adopt: $V_{\rm HB} = 18.10 \pm 0.05$ mag, E(B-V) = 0.01 mag and $(m-M)_V = 17.37$ mag (Harris 1996). From these values, the mean ridgeline listed in Table 4, and the location of the RGB "bump" from BCSS97, we derive: $(B-V)_{0,\rm g} = 0.84 \pm 0.03$ mag, $\Delta V_{1.1} = 1.54 \pm 0.07$ mag,

 $\Delta V_{1.2} = 1.95 \pm 0.07$ mag, $\Delta V_{1.4} = 2.56 \pm 0.07$ mag, $(B-V)_{0,-2} = 1.47 \pm 0.05$ mag, $S = 4.62 \pm 0.07$, and $\Delta V_{\rm bump}^{\rm HB} = -0.05 \pm 0.08$ mag.

An additional estimate of the cluster metallicity can be derived by the so-called "simultaneous reddening and metallicity (SRM) method" (Sarajedini 1994; Sarajedini & Layden 1997). This method was created to derive the reddening and metallicity of a GC simultaneously from its RGB and HB photometric properties.

From each of these observables we can obtain an independent *photometric* estimate of the cluster metallicity by using the corresponding calibration in terms of [Fe/H] reported in the literature. Most of the available calibrations are based on the Zinn & West (1984, hereafter ZW84) metallicity scale, although some recent papers (Carretta & Bragaglia 1998; Ferraro et al. 1999a) have presented recalibrations in terms of the new scale by Carretta & Gratton (1997, hereafter CG97), based on direct high-resolution spectroscopy for RGB stars in a set of 24 GCs.

Results based on each available metallicity indicator on the two metallicity scales are summarized in Table 7.

We note that the reddening obtained from the SRM method based on the Sarajedini & Layden (1997) calibration, $E(B-V)=0.02\pm0.01$ mag, is fully consistent with the values commonly found in the literature (e.g., Harris 1996).

On the Zinn & West (1984) scale, the weighted mean photometrically-inferred NGC 6229 metallicity is:

$$[Fe/H]_{ZW84 \text{ scale}} = -1.4 \pm 0.1 \text{ dex.}$$
 (3)

Instead, on the $Carretta\ \mathcal{C}\ Gratton\ (1997)\ scale$ the NGC 6229 metallicity is:

$$[Fe/H]_{CG97 \text{ scale}} = -1.1 \pm 0.1 \text{ dex.}$$
 (4)

Note that the quoted uncertainties in the metallicity estimates provided in Table 7 are derived only from the formal propagation of the errors in the photometric indicators. However, in the final values we assume a conservative global error of 0.1 dex.

It is important to note that a substantially lower metallicity ($[M/H] = -1.4 \pm 0.1$) than provided in the CG97 scale (eq. 4) has recently been obtained for NGC 6229 from direct medium-resolution spectroscopy of bright cluster giants (Wachter et al. 1998).

However, particular care is required in comparing different metallicty scales, since most of them are found not to be mutually consistent. Carretta & Gratton (1998) noted that in the Wachter et al. (1998) scale Galactic GCs turn out to be systematically more metal poor with respect to the CG97 scale. In fact, considering two clusters (namely, M 13 and NGC 7006) examined with both the Wachter et al. and CG97 techniques, they found:

$$[Fe/H]_{CG97 \text{ scale}} = [M/H]_{Wachter \text{ et al. scale}} + 0.2 \text{ dex.}$$

Taking into account this offset, the metallicity found by Wachter et al. (1998) for NGC 6229 translates into a value

$$[\text{Fe/H}]_{\text{CG97 scale}} = -1.2 \pm 0.1 \text{ dex}$$

in the CG97 scale, which is fully compatible with the photometric estimate we found above (see eq. 4). Note that Pilachowski et al. (1983) derived [Fe/H] $\simeq -1.3$ from echelle spectroscopy of a red giant (IV-12) in NGC 6229; in their scale, however, 47 Tuc (NGC 104) had a surprisingly low metallicity ([Fe/H] = -1.09), thus indicating that the "true" NGC 6229 metallicity should be higher than implied by the ZW84 scale.

Since the CMDs of NGC 6229 and M 5 agree remarkably well at the level of the RGB, the two clusters must have essentially identical (photometric) metallicities. This conclusion does not depend upon (possible) deep mixing effects among NGC 6229's and/or M 5's giants, since mixing affects only marginally the RGB locus and shape (Sweigart 1997).

Thus we can conclude that both spectroscopic and photometric measurements suggest that M 5's (and thus NGC 6229's) metallicity is indeed quite high: $[Fe/H] = -1.1 \pm 0.1$ (see also Sneden et al. 1992).²

5. Age determination

As already stated, our photometric material allowed us to obtain, for the first time, a CMD for NGC 6229 reaching below the cluster TO point and suitable for an age determination. In Figure 4, the cluster CMD obtained from the CA dataset is displayed together with the M5 ridgeline from Sandquist et al. (1996). Note that a comparison between the outer-halo GC NGC 6229 and M5 appears especially interesting in light of the discovery that M5's orbital parameters imply that it too is an outer-halo GC, which just happens to be currently close to its perigalacticon (Cudworth 1997 and references therein).

Comparing the NGC 6229 CMD with the one for M 5, we reach the following conclusions.

Assuming that M5 and NGC 6229 have the same metallicity (see Sect. 4) and using the remarkable fit of

Table 7. Metallicity of NGC 6229

Parameter	[Fe/H]	Reference
Zir	nn & West (1984)	metallicity scale
$(B - V)_{0,g}$	-1.39 ± 0.15	Zinn & West (1984)
	-1.40 ± 0.13	Gratton (1987)
	-1.26 ± 0.13	Costar & Smith (1988)
	-1.37 ± 0.10	Gratton & Ortolani (1989)
	-1.36 ± 0.15	Sarajedini & Layden (1997)
	-1.36 ± 0.05	$Weighted\ mean$
$\Delta V_{1.4}$	-1.45 ± 0.07	Zinn & West (1984)
	-1.29 ± 0.07	Costar & Smith (1988)
	-1.38 ± 0.05	Gratton & Ortolani (1989)
	-1.37 ± 0.04	$Weighted\ mean$
$\Delta V_{1.1}$	-1.33 ± 0.06	Sarajedini & Layden (1997)
$\Delta V_{1.2}$	-1.33 ± 0.06	Sarajedini & Layden (1997)
$(B-V)_{0,-2}$	-1.31 ± 0.05	Sarajedini & Layden (1997)
S	-1.35 ± 0.05	Gratton & Ortolani (1989)
$\Delta V_{ m bump}^{ m HB}$	-1.40 ± 0.10	Sarajedini & Forrester (1997)
"SRM method"	-1.44 ± 0.08	Sarajedini & Layden (1997)
Carret	ta & Gratton (19	997) metallicity scale
$(B-V)_{0,g}$	-1.12 ± 0.08	Carretta & Bragaglia (1998)
$\Delta V_{1.1}$	-1.06 ± 0.08	Carretta & Bragaglia (1998)
$\Delta V_{1.2}$	-1.10 ± 0.08	Carretta & Bragaglia (1998)

the M5 ridgeline to the NGC 6229 CMD in the SGB-TO region (see Figure 4), it immediately follows that M 5 and NGC 6229 have very similar ages (VandenBerg et al. 1990). A similar conclusion follows from a comparison with the NGC 1851 ridgeline (Walker 1992; see also Figure 7 in Walker 1998). Figure 4 shows, however, that the match between the HBs is not very good at the red end of the blue HB, which appears brighter in NGC 6229 than in M5. The red-HB loci agree quite well, though. (A comparison between the RR Lyrae properties is deferred to Paper IV in our series.) This is similar to what has been claimed by Stetson et al. (1996) for the bimodal-HB cluster NGC 1851. BCSS97 had already hinted that the red end of the blue HB of NGC 6229 might be brighter than the red HB of the cluster (see also Figure 6). Figure 9a shows a more detailed comparison between the NGC 6229 and M 5 CMDs around the TO and HB regions. That the blue HB of NGC 6229 is brighter than M 5's is quite evident in this plot. The same is not true when a comparison is made between NGC 6229 and NGC 1851, however (Figure 9b). This may shed light on the nature of the secondparameter effect (Stetson et al. 1996; Catelan et al. 1998; Sweigart 1999; Sweigart & Catelan 1998; Walker 1998).

To confirm quantitatively that NGC 6229 and M 5 are essentially coeval, we have applied both "vertical" and "horizontal" methods for determining relative ages from the magnitude difference $\Delta V_{\rm TO}^{\rm HB}$ between the HB and the TO and the color difference $\Delta (B-V)_{\rm TO}^{\rm RGB}$ between the RGB and the TO. In order to overcome the problems related to the calibration and use of absolute quantities, we have applied these age parameters in a strictly differential sense by referring NGC 6229 to our reference GC M 5, fol-

 $^{^2}$ It is interesting to note that, according to the latest isochrones computed by VandenBerg (1998), it is not possible to fit M5's CMD unless [Fe/H] <-1.3 (even including the observed enhancement in the $\alpha\text{-}\text{elements};$ Sneden et al. 1992), thus favoring the ZW84 scale. On the other hand, assuming the "global metallicity" [M/H] and adopting the latest models by Chieffi et al. (1998), Ferraro et al. (1999a) have been able to remove the disagreement between theory and observations in regard to the location of the RGB luminosity function "bump" (e.g., Fusi Pecci et al. 1990) in a sample of 47 Galactic GCs – favoring instead the CG97 scale. Possible explanations for the discrepancy between theory and observations, as far as the "bump" location goes, have been summarized by Catelan & de Freitas Pacheco (1996; see their Sect. 5).

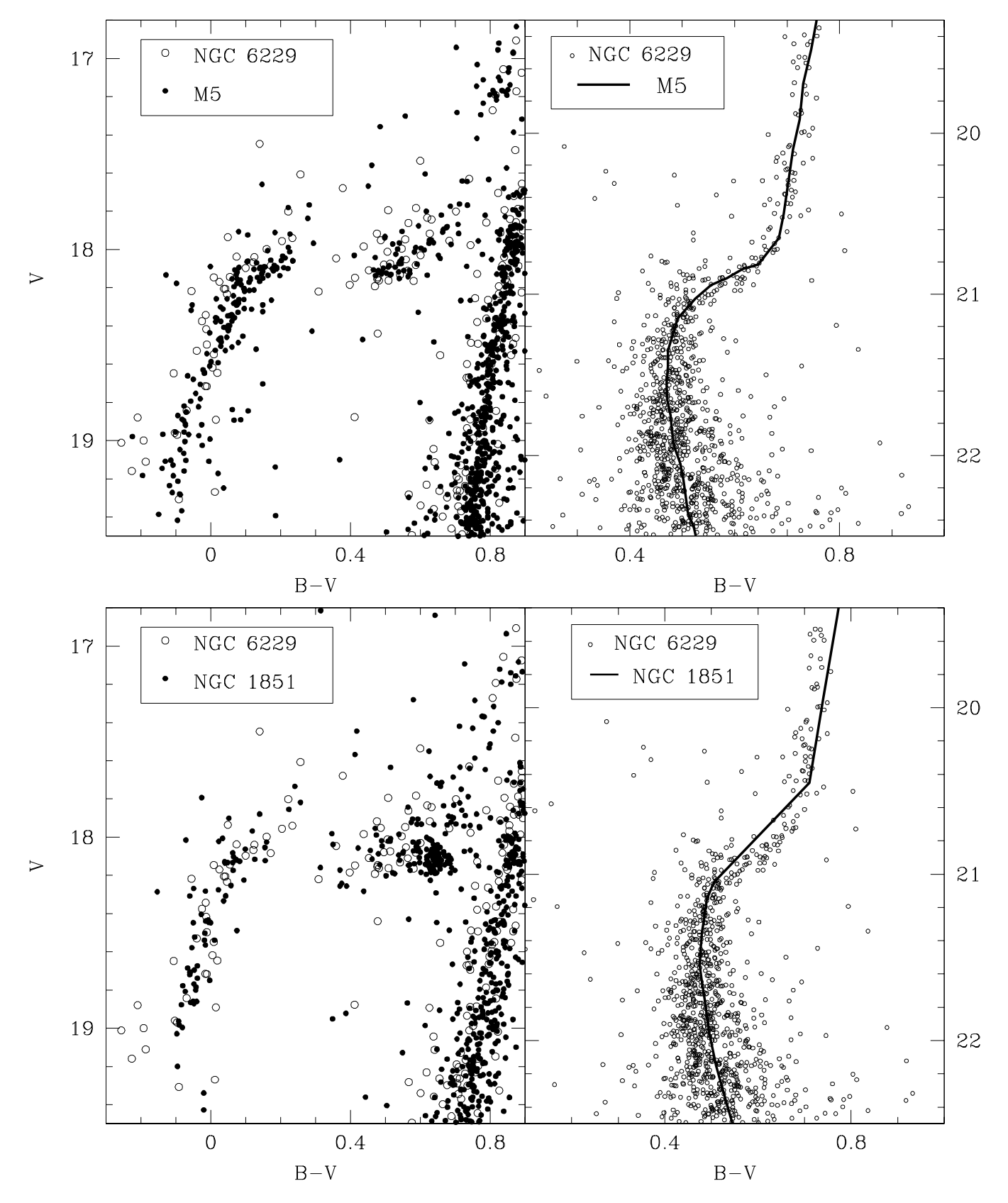


Fig. 9. a) Detailed comparison between the NGC 6229 and M 5 CMDs: in the left-hand panel the HB region for stars from the CA dataset with 32'' < r < 75'' has been plotted. In the right-hand panel, the SGB-TO region for stars from the CA dataset with r > 75'' has been plotted. The solid line represents the M 5 ridgeline from Sandquist et al. (1996). b) Same as a), except that NGC 1851 has been used for a comparison (data from Walker 1992). Open circles represent NGC 6229 and filled circles either M 5 or NGC 1851. In both panels, known variables have been removed

lowing the approach of Buonanno et al. (1993) and I. Ferraro et al. (1995).

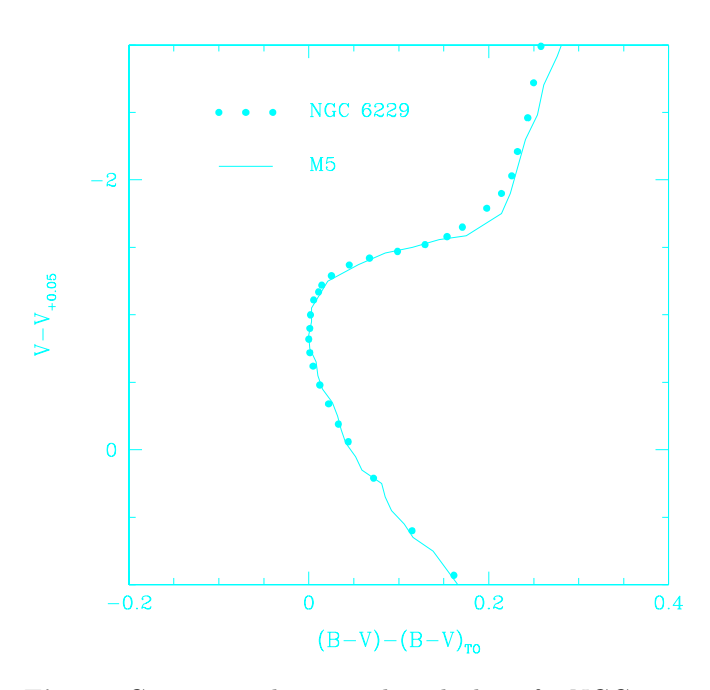


Fig. 10. Comparison between the ridgelines for NGC 6229 (\bullet) and M 5 (-), registered following the VandenBerg et al. (1990) prescriptions in order to obtain a measurement of their relative ages

On the basis of the VandenBerg & Bell (1985) models, Buonanno et al. (1993) obtained the following "vertical" relation between the differential age parameter $\Delta = \Delta_1 V_{\rm TO}^{\rm HB} - \Delta_2 V_{\rm TO}^{\rm HB}$ and the age t_9 in Gyr:

$$\Delta \log t_9 = (0.44 + 0.04 \, [\text{Fe/H}]) \, \Delta$$

where subscript "1" stands for NGC 6229, and "2" for M 5. Assuming [Fe/H] ~ -1.1 for both GCs and using the value of $\Delta V_{\rm TO}^{\rm HB}$ derived in Sect. 3.1 for NGC 6229, we obtained: $\Delta = 3.50 - 3.47 = 0.03 \pm 0.13$ mag, implying $\Delta \log t_9 \sim 0.0119$ and thus

$$\Delta t_9 (\text{NGC } 6229 - \text{M } 5) \sim +0.4 \pm 2.0 \text{ Gyr.}$$

The "horizontal" method has been applied following the procedure described by VandenBerg et al. (1990). In Figure 10 we compare the M5 and NGC 6229 fiducial lines after registering them as recommended by VandenBerg et al. According to that paper the colour difference $\Delta(B-V)_{\mathrm{TO}}^{\mathrm{RGB}}$ is computed at the point along the RGB where $V-V_{+0.05}=-2.5$ mag. Here $V_{+0.05}$ is the MS magnitude at which B-V is 0.05 mag redder than the TO. From Figure 10 we derive a value of -0.010 ± 0.015 for the differential age parameter $\delta=\Delta_1(B-V)_{\mathrm{TO}}^{\mathrm{RGB}}-\Delta_2(B-V)_{\mathrm{TO}}^{\mathrm{RGB}}$, defined by Buonanno et

al. (1993). Using the calibration of δ given by VandenBerg & Stetson (1991), namely,

$$\Delta \log t_9 = (-4.32 - 0.78 \, [\text{Fe/H}]) \, \delta$$

we obtain an age difference between NGC 6229 and M 5 of

$$\Delta t_9 (\text{NGC } 6229 - \text{M } 5) \sim +1.2 \pm 1.5 \text{ Gyr.}$$

A new age parameter has been recently defined by Buonanno et al. (1998): $\Delta V^{0.05}$, which is the magnitude difference between the HB and the point on the upper MS, where B-V is 0.05 mag redder than the TO (see Figure 1 in Buonanno et al.). For M 5 and NGC 6229, we find that: $\Delta V^{0.05} = 4.31 \pm 0.10$ mag and 4.32 ± 0.11 mag, respectively. This implies an age difference

$$\Delta t_9 (\text{NGC } 6229 - \text{M } 5) \sim +0.1 \pm 1.5 \text{ Gyr}$$

between these two GCs.

In summary, all the employed methods agree within the errors that NGC 6229 and M 5 are essentially coeval.³

The weighted mean age difference between NGC 6229 and M 5 from the three determinations is:

$$\Delta t_9 (\text{NGC } 6229 - \text{M } 5) \simeq +0.5 \pm 1.0 \text{ Gyr.}$$
 (5)

For a comparison of the age of M 5 with those of other GCs of comparable metallicity, we refer the reader to Vanden-Berg et al. (1990) and VandenBerg (1999b).

6. Summary and concluding remarks

In the present paper we have presented the first deep CMD for the outer-halo globular cluster NGC 6229 from data obtained at the Calar Alto and Rozhen observatories. The combined CMD reaches ~ 2 mag below the main-sequence turnoff of the cluster.

Our detailed analysis of the CMD properties reveals that:

1. The perfect alignment of the upper RGBs in NGC 6229 and M 5 suggests that they must have the same metallicity. This is confirmed by our *photometric* estimate of NGC 6229's metallicity ([Fe/H]_{CG97 scale} = -1.1 ± 0.1 dex), which fully agrees with the spectroscopic measurements obtained by CG97 and Sneden et al. (1992) for M 5 ([Fe/H]_{CG97 scale} = -1.1 ± 0.1 dex, $[\alpha/\text{Fe}] \simeq +0.2$ dex).

 $^{^3}$ In the present paper, we have chosen not to employ the recently-proposed relative-age indicator from Chaboyer et al. (1996a), which relies on the region of the CMD which is brighter than the TO and redder by 0.05 mag in B-V. We find that this region is particularly subject to spurious photometric blends (Sect. 3.1), and thus – unlike what is claimed by Chaboyer et al. – is subject to potentially large observational errors.

Our photometric estimate of the NGC 6229 metallicity has been indirectly confirmed by the recent spectroscopic measurements carried out by Wachter et al. (1998), who found $[M/H] = -1.4 \pm 0.1$ dex. Once the offset between the Wachter et al. and CG97 metallicity scales found for GCs in common between the two studies is properly taken into account (Carretta & Gratton 1998), this corresponds to $[Fe/H]_{CG97 \text{ scale}} = -1.2 \pm 0.1 \text{ dex}$;

- 2. The CMD of NGC 6229 is entirely compatible with the one for M 5 (Sandquist et al. 1996), implying that the two clusters have nearly identical ages. Indeed, a quantitative measurement of the age difference between the two GCs using three different methods shows them to have the same ages to within ≈ 1 Gyr. However, the HB morphologies of the two clusters do differ in detail, NGC 6229's extending to bluer colours than M 5's (with a likely extreme HB population present) and showing a "dip" in the number counts at the RR Lyrae level (see the Appendix in Catelan et al. 1998 for a discussion);
- 3. Thirty-three candidate blue straggler stars have been identified;
- 4. Nine possible extreme HB stars have been detected. If confirmed, this will be the first known case of an outer-halo GC with an extreme HB population. Associated with this population, we find a hint of a (second) "gap" at the faint end of the blue HB. NGC 6229 is the only known outer-halo globular with HB gap(s) and a bimodal HB (BCSS97; Catelan et al. 1998);
- 5. Confirmation of the BSS and EHB populations, as well as a detailed analysis of the radial population gradients discussed by BCSS97 and in Sect. 5.2, must await deep HST photometry of the crowded central regions of this remote and quite concentrated globular cluster.

Acknowledgements. The authors are grateful to E. Carretta, R. Gratton, F. Grundahl, D. A. VandenBerg and the referee, B. Carney, for very helpful remarks. This research was supported in part by the Bulgarian National Science Foundation grant under contract No. F-604/1996 with the Bulgarian Ministry of Education and Sciences. Support for M.C. was provided by NASA through Hubble Fellowship grant HF-01105.01-98A awarded by the Space Telescope Science Institute, which is operated by the Association of Universities for Research in Astronomy, Inc., for NASA under contract NAS 5-26555.

References

Bolte M., 1990, JRASC 84, 137

Borissova J., Catelan M., Spassova N., Sweigart A. V., 1997, AJ 113, 692 (BCSS97)

Buonanno R., Buscema G., Corsi C. E., Ferraro I., Iannicola G., 1983, A&A 126, 278

Buonanno R., Corsi C. E., Fusi Pecci F., 1985, A&A 145, 97 Buonanno R., Corsi C. E., Fusi Pecci F., Richer H. B., Fahlman G. G., 1993, AJ 105, 184

Buonanno R., Corsi C. E., Pulone L., Fusi Pecci F., Bellazzini M., 1998, A&A 333, 505

Buzzoni A., Fusi Pecci F., Buonanno R., Corsi C. E., 1983, A&A 128, 94

Carney B., Fullton L., Trammell S., 1991, AJ 101, 1699

Carretta E., Bragaglia A., 1998, A&A 329, 937

Carretta E., Gratton R., 1997, A&AS 121, 95 (CG97)

Carretta E., Gratton R., 1998, private communication

Catelan M., 1999, in preparation

Catelan M., Borissova J., Sweigart A. V., Spassova, N., 1998, ApJ 494, 265

Catelan M., de Freitas Pacheco J. A., 1996, PASP 108, 166

Chaboyer B., Demarque P., Kernan P. J., Krauss L. M., Sarajedini A., 1996a, MNRAS 283, 683

Chaboyer B., Demarque P., Sarajedini A., 1996b, ApJ 459, 558 Chieffi A., Limongi M., Straniero O., 1998, in preparation

Christian C., Adams M., Barnes J. V. Hayes, D. S., Siegel M., Butcher H., Mould J. R., 1985, PASP 97, 363

Cohen J. G., 1986, AJ 90, 2254

Costar D., Smith H. A., 1988, AJ, 96, 1925

Cudworth K. M., 1997, in Proper Motions and Galactic Astronomy, ASP Conf. Ser. Vol. 127, ed. R. M. Humphreys, ASP, San Francisco, 91

Ferraro F. R., Clementini, G., Fusi Pecci, F., Buonanno, R., Alcaino, G. 1990, A&AS 84, 59

Ferraro F. R., Fusi Pecci F., Buonanno R. 1992, MNRAS 256, $376\,$

Ferraro F. R., Fusi Pecci F., Bellazzini M., 1995, A&A 294, 80 Ferraro F. R., Messineo M., Fusi Pecci F., De Palo M. A., Straniero O., Chieffi A., 1999a, AJ, submitted

Ferraro F. R., Paltrinieri B., Fusi Pecci F., et al., 1997, A&A 324, 915

Ferraro F. R., Paltrinieri B., Fusi Pecci F., Rood R. T., Dorman B., 1998, ApJ 500, 311

Ferraro F. R., Paltrinieri B., Rood R. T., Dorman B., 1999b, ApJ (Letters), submitted

Ferraro F. R., Paresce F., 1993, AJ 106, 154

Ferraro I., Ferraro F. R., Fusi Pecci F., Corsi C. E., Buonanno R., 1995, MNRAS 275, 1057

Fusi Pecci F., Ferraro F. R., Cacciari C., 1993, in *Blue Stragglers*, ASP Conf. Ser. Vol. 53, ed. R. E. Saffer, ASP, San Francisco, 97

Fusi Pecci F., Ferraro F. R., Corsi C. E., Cacciari C., Buonanno R., 1992, AJ 104, 1831

Fusi Pecci F., Ferraro F. R., Crocker D. A., Rood R. T., Buonanno R., 1990, A&A 238, 95

Gratton R. G., 1987, A&A 179, 181

Gratton R. G., Ortolani S., 1989, A&A 211, 41

Harris W. E., 1996, AJ 112, 1487

Harris W. E., et al., 1997, AJ 114, 1043

Hartwick F. D. A., 1968, ApJ 154, 475

Iben I., Jr., 1968, Nature 220, 143

Pilachowski C. A., Bothun G. D., Olszewski E. W., Odell A., 1983, ApJ 273, 187

Ratnatunga K., Bahcall J., 1985, ApJS 58, 63

Rood R. T., Crocker D. A., Fusi Pecci F., Ferraro F.
R., Clementini G., Buonanno R., 1993, in *The Globular Cluster-Galaxy Connection*, ASP Conf. Ser. Vol. 48, eds.
G. H. Smith & J. P. Brodie, ASP, San Francisco, 218

Sandage A. R., Wallerstein G., 1960, ApJ 131, 598

Sandage A. R., Smith L. L., 1966, ApJ 144, 886

Sandquist E. L., Bolte M., Stetson P. B., Hesser J. E., 1996, ApJ 470, 910

Sarajedini A., 1994, AJ 107, 618

Sarajedini A., 1997, AJ, 113, 682

Sarajedini A., Forrester W. L., 1995, AJ 109, 1112

Sarajedini A., Layden A., 1997, AJ 113, 264

Sneden C., Kraft R. P., Prosser C. F., Langer G. E., 1992, AJ 104, 2121

Sosin C., et al., 1997, ApJ 480, L35

Stetson P. B., 1991a, in The Formation and Evolution of Star Clusters, ASP Conf. Ser. Vol. 13, ed. K. A. Janes, ASP, San Francisco, 88

Stetson P. B., 1991b, in Precision Photometry: Astrophysics of the Galaxy, eds. A. G. D. Philip, A. R. Upgren, & K. A. Janes, L. Davis Press, Schenectady, 69

Stetson P. B., 1993, User's Manual for DAOPHOT II

Stetson P. B., et al., 1999, AJ, in press (astro-ph/9809176)

Stetson P. B., Harris W. E., 1988, AJ 96, 909

Sweigart A. V., 1997, ApJ 474, L23

Sweigart A. V., 1999, in The Third Conference on Faint Blue Stars, eds. A. G. D. Philip, J. Liebert, & R. A. Saffer, Cambridge University Press, Cambridge, 3

Sweigart A. V., Catelan M., 1998, ApJ 501, L63

Trager S. C., King I. R., Djorgovski S., 1995, AJ 109, 218

VandenBerg D. A., 1998, private communication

VandenBerg D. A., 1999a, in *The Third Stromlo Symposium: The Galactic Halo*, ASP Conf. Ser., eds. B. K. Gibson, T. S. Axelrod, & M. E. Putman, ASP, San Francisco, in press

VandenBerg D. A., 1999b, in preparation

VandenBerg D. A., Bell R. A., 1985, ApJS 58, 561

VandenBerg D. A., Bolte M., Stetson P. B., 1990, AJ 100, 445

VandenBerg D. A., Stetson P. B., 1991, AJ 102, 1043

Wachter S., Wallerstein G., Brown J. A., Oke J. B., 1998, PASP 110, 821

Walker A. R., 1992, PASP 104, 1063

Walker A. R., 1998, AJ 116, 220

Zinn R., West M., 1984, ApJ 55, 45 (ZW84)